Published in final edited form as:
J Vasc Interv Radiol. 2008 October ; 19(10): 1483–1489. doi:10.1016/j.jvir.2008.06.017.

Comparison of Hypoxia-inducible Factor-1 alpha Expression Before and After Transcatheter Arterial Embolization in Rabbit VX2 Liver Tumors

Sumeet Virmani, MD[1], **Thomas K. Rhee, MD**[1], **Robert K. Ryu, MD**[1], **Kent T. Sato, MD**[1], **Robert J. Lewandowski, MD**[1,2], **Mary F. Mulcahy, MD**[1,2,3], **Laura M. Kulik, MD**[1,3], **Barbara Szolc-Kowalska, MD**[4], **Gayle E. Woloschak, PhD**[2,4], **Guang-Yu Yang, MD, PhD**[2,5], **Riad Salem, MD, MBA**[1,2], **Andrew C. Larson, PhD**[1,2,6], and **Reed A. Omary, MD, MS**[1,2,6]

1*Department of Radiology, Northwestern University, Chicago, IL 60611*

2*Robert H. Lurie Comprehensive Cancer Center, Northwestern University, Chicago, IL 60611*

3*Department of Medicine, Northwestern University, Chicago, IL 60611*

4*Department of Radiation Oncology, Northwestern University, Chicago, IL 60611*

5*Department of Pathology, Northwestern University, Chicago, IL 60611*

6*Department of Biomedical Engineering, Northwestern University, Chicago, IL 60611.*

Abstract

Purpose—Hypoxia-inducible factor-1 alpha (HIF-1 α) expression has been linked with increased mortality and treatment failure in various cancers. The purpose of this study was to test the hypothesis that transcatheter arterial embolization (TAE) induces expression of HIF-1 α within the same rabbit VX2 liver tumor.

Materials and Methods—Seven VX2 tumors were grown in the livers of 5 New Zealand white rabbits. Ultrasound guided biopsies were taken before and 10 min after TAE from all tumors. Pre- and post- TAE tumor biopsy specimens along with post- TAE whole liver tumor sections were stained with HIF-1 α antibody and analyzed for percentage of HIF-1 α positive nuclei using a spectral unmixing system mounted on a high powered microscope. Statistical data comparisons were performed using Wilcoxon signed-rank test (alpha=0.05).

Results—TAE of liver tumors resulted in a statistically significant increase in the mean percentage of HIF-1 α expression. The mean percentage of HIF-1 α positive stained nuclei increased from 23 % ± 3.5% in pre- TAE biopsy specimens to 41% ± 8.7% ($p< 0.02$) in post- TAE biopsy specimens. The increase was even more significant when mean percentage of HIF-1 α positive stained nuclei from the same pre- TAE biopsy specimens were compared to sections from post- TAE whole tumor specimens [60% ± 8.9% ($p<0.02$)].

Address Correspondence to: Reed A Omary, MD, MS, Department of Radiology, Northwestern University, 737 N Michigan Avenue, Suite 1600, Chicago, IL 60611, E-mail: reed@northwestern.edu, Tel: (312)-695-3774, Fax: (312)-926-0826.

Disclosures:
None of the authors have identified a conflict of interest.

Conclusions—The study revealed that hypoxia caused by TAE of VX2 liver tumors activates HIF-1 α, a transcription factor that in turn regulates other pro-angiogenic factors.

Introduction

Hepatocellular carcinoma (HCC) is the 5th leading cause of cancer death in the world (1). Developed countries, including the U.S., have had an 80% increase in HCC incidence over the last 15–20 years. Surgical resection and liver transplantation are the sole potentially curative HCC treatments, but only 10–15% of patients are surgical candidates (2). Hence, most other systemic and regional therapies offer palliation rather than cure. Transcatheter arterial embolization (TAE) and transcatheter arterial chemoembolization (TACE) are widely used palliative treatments for patients with primary and/or metastatic malignant liver tumors and has shown encouraging results in terms of survival (3). The rationale for TAE is based on obstructing the blood flow to the tumor and inducing tumor necrosis while preserving adequate liver function.

It is generally accepted that TAE rarely achieves total necrosis of the targeted liver tumor and some reports (4,5) even suggest that TAE may actually accelerate the rate of intrahepatic or extrahepatic metastasis. The underlying molecular mechanisms for some treatment failures have been linked to neovascularization and angiogenesis (4,6,7). To increase nutrients and oxygen supply, the residual surviving tumor cells secrete several angiogenic factors. In 1992, Semenza et al (8) discovered that Hypoxia inducible Factor-1 α (HIF-1 α) was a control factor regulating the subsequent release of multiple angiogenic factors (Figure 1) (9), including Vascular Endothelial Growth Factor (VEGF), basic fibroblast growth factor (bFGF) and insulin like growth factor (IGF). During TAE, stasis to forward blood flow creates hypoxic conditions and may promote tumor angiogenesis (6,10) by inducing expression of HIF-1 α (11).

HIF-1 α has been linked with increased mortality and treatment failure in various cancers; however its role in HCC, especially its behavior after TAE is poorly understood. An initial study by Rhee et al (11) suggested that TAE increases HIF-1 α expression, but all the experiments were compared with non embolized controls from separate VX2 liver tumor rabbits. Our study was performed to address this limitation and tests the hypothesis that TAE induces expression of HIF-1 α within the same rabbit VX2 liver tumor.

Material and Methods

Animal model and Tumor Implantation

Our institutional animal care and use committee approved all the experiments and were performed in accordance with institutional guidelines. All procedures were performed on 7 New Zealand white rabbits weighing approximately 4–5kg. We used the rabbit VX2 carcinoma liver tumor model because of the similarity of its blood supply to human HCC and because rabbit hepatic arteries are sufficiently large enough to permit hepatic artery catheterizations (12).

All procedures were performed on 7 rabbits (n = 2 donor; n = 5 recipient) under anesthesia and sterile conditions. VX2 cells were initially implanted in both hind limbs of two donor rabbits. Each of these two rabbits received 0.75–1.0mL of freshly prepared VX2 cell solution in the gluteal muscles of the hind limbs (13). After 4 weeks of tumor growth, hind limb tumors were harvested and small tumor fragments (1–2 mm in diameter) were dissected from the viable tumor tissue. For surgical VX2 liver tumor implantations, each of the 5 additional rabbits were anesthetized with intramuscular (IM) ketamine 44 mg/kg, xylazine 3–5 mg/kg and administered inhaled isofluorane 2–3% as needed. These tumor fragments were then immediately implanted in the left lobe of liver in each recipient rabbit via a mini-laparotomy

performed in the subxiphoid area (13). Two tumor fragments each were implanted in the liver parenchyma of all the 5 rabbits. Tumors were implanted 4–5 cm apart and 2 cm deep. Gentle pressure was applied to arrest any bleeding and a small (1×1 cm^2) piece of Surgicel (Ethicon, Johnson & Johnson, Somerville, New Jersey) was placed over the incision sites on the liver. The abdomen was closed in three layers. Liver tumors were incubated for three weeks before imaging.

MRI

MRI was performed using a 1.5 T Magnetom Sonata clinical MRI scanner (Siemens Medical Solutions, Erlangen, Germany). Three weeks after tumor implantation, each rabbit underwent MRI to detect tumor growth. Rabbits were anesthetized with IM ketamine 44 mg/kg and xylazine 3–5 mg/kg. They were then imaged in supine position using a flexible surface coil. Tumor growth was considered positive when tumor was identified in axial and sagittal imaging planes by two independent MR imaging specialists. Anatomic images of the hind limb or liver tumors in all 7 rabbits were acquired using a T2-weighted turbo spin-echo (T2W TSE) sequence with the following imaging parameters: TR/TE = 3000/82 milliseconds, 4-mm slice thickness, 130-Hz/pixel BW, 200×100 mm^2 field of view, 256×126 matrix ($0.8 \times 0.8 \times 4.0$-mm^3 voxel size), turbo factor = 7, averages = 4.

X-ray Digital Subtraction Angiography (DSA)

During hepatic artery catheter placement, x-ray DSA was performed using a Siemens C-arm PowerMobil unit (Siemens Medical Solutions, Erlangen, Germany). All 5 rabbits with VX2 liver tumors were anesthetized using a mixture of IM ketamine (80mg/kg) and xylazine (5mg/kg). Inhalational isoflurane (2–3.5%) was administered for anesthesia through an endotracheal tube with a small animal ventilator (Harvard Apparatus, Holliston, MA, USA), if required. We surgically cut down on the femoral artery and then introduced a 3-F vascular sheath (Cook, Bloomington, IN, USA). A 2-F catheter (JB-1, Cook, Bloomington, IN) was advanced superselectively over a 0.014-inch diameter guidewire into the left hepatic artery that supplied the targeted tumor. Before TAE, DSA of the left hepatic artery was performed using 2 ml manual injections of full strength Omnipaque 350 (Amersham, Princeton, NJ). The catheter was secured in its selected position using a 2-0 silk suture in rabbit's groin. After TAE, we confirmed reduction in antegrade blood flow to the liver tumors with DSA of the left hepatic artery.

TAE

We used 40–120 μm diameter Embosphere® (BioSphere Medical TM, Rockland MA), as our embolic agent for TAE. These hydrophilic beads contain an acrylic co-polymer cross-linked with gelatin (14). Embospheres® are supplied in pre-filled syringes containing 2mL of particles (16 million spheres) mixed in 6mL of saline solution (total solution 8mL/pre-filled syringe). Each syringe was diluted with a saline and iodinated contrast agent (Omnipaque 350, Amersham, Princeton, NJ) mixture to yield ~250,000 microspheres/mL. For each TAE, Embospheres® were super-selectively delivered by hand injection through the same catheter previously placed during DSA. All TAEs using Embosphere® were performed until complete stasis of antegrade blood flow for all 5 liver tumor rabbits. The endpoint "stasis" was defined as elimination of any tumor blush and antegrade arterial flow distal to catheter tip. This corresponded to a subjective angiographic chemoembolization endpoint (SACE) level of IV (15).

Ultrasound-guided tumor biopsy

Ultrasound of the liver tumors was performed using a 5-megahertz abdominal transducer. All rabbits underwent percutaneous ultrasound-guided core needle biopsies of the targeted VX2

liver tumors using 18-gauge needles (US Biopsy, Franklin, IN). The 15 cm long biopsy needle had a 15mm throw to obtain biopsy samples. Biopsies were taken before and 10 min after TAE from all liver tumors and were immediately collected in 10% formalin saline. A minimum of 3 tumor biopsy samples were taken and were obtained from the periphery of tumors from different regions.

Necropsy

Each rabbit was sacrificed with an intravenous injection of 150–200 mg/kg sodium pentobarbital (Euthasol; Delmarva Laboratories, Midlothian, VA) once the post- TAE biopsies were completed. All 5 rabbits were euthanized for tumor confirmation at gross necropsy. Liver specimens were removed and placed in 10% neutral buffered formalin for fixation.

HIF-1 alpha immunohistochemical staining

All harvested liver specimens and pre- as well as post- TAE biopsy specimens were kept in 10% neutral buffered fomalin for 72 hrs. Once fixed, liver tumors were removed en bloc and then sliced along the axial plane. Samples were embedded in paraffin, and a 4-um thick slice was cut from the whole tumor slices as well as biopsy specimens and mounted on glass slides. Paraffin sections were dewaxed and washed with hydrogen peroxide for 5 minutes and then rinsed gently with distilled water. The slides were then blocked with protein at room temperature for 5 minutes. These sections were stained with mouse anti HIF-1 α IgG2b monoclonal antibody (NB100-123, Novus Biologicals, Littleton, CO; dilution, 1: 40,000) for 15 minutes. After 15 minutes, slides were washed with freshly prepared Tris-Buffered Saline Tween (TBST) solution three times for 3–5 minutes each. Slides were then incubated with a secondary anti mouse immunoglobulin – HRP and then washed with TBST solution three times for 3–5 minutes each. Hematoxylin was used as a nuclear counterstain.

Data Analysis

All slides were reviewed under light microscopy by a non-blinded board-certified attending surgical pathologist with over 10 years experience. Pre- and post- TAE tumor biopsy specimens along with post- TAE whole liver tumor sections were stained with anti mouse HIF-1 α monoclonal antibody and analyzed for percentage of HIF-1 α positive nuclei using the Nuance spectral unmixing system mounted on a Zeiss Axioskop 50 microscope. Statistical data comparisons were performed by using a non-parametric Wilcoxon signed-rank test (alpha=0.05; non-directional). All data are denoted as mean ± standard deviation. Analysis was performed separately for post- TAE tumor biopsy specimens as well as for post-TAE whole tumor specimens.

Results

Of the 10 separate tumor implantations, seven VX2 liver tumors were successfully grown in a total of 5 rabbits. Tumor location was successfully depicted as regions of increased signal intensity on T2-w TSE MRI (Figure 2a). Tumors varied from 1.5 to 2.5 cm in diameter (mean 1.9 cm).

All targeted tumors were successfully catheterized and could be visualized as a region of hypervascular blush under DSA. As would be expected, this blush was typically more intense in the more viable, peripheral portion of the tumor. On ultrasound, VX2 liver tumors appeared iso- to hypoechoic. The tumors were successfully biopsied pre- and post- TAE using an 18-gauge core biopsy needle under ultrasonographic guidance (Figure 2b). No complications were observed during the procedures. Representative pre- and post- TAE DSA images following iodinated contrast injection into the left hepatic artery are shown in Figure 3a and 3b. Post-

TAE DSA confirmed successful reduction in blood flow to tumors. None of the harvested tumors showed any evidence of significant hemorrhage or arteriovenous fistula (Figure 4).

At microscopic examination, normal rabbit liver parenchyma was seen as symmetrically arranged anastomosing sheets of hepatocytes. The VX2 tumor margins were well defined and consisted of areas of densely packed tumor cells intermixed with areas of necrotic cells. The necrotic cells were identified by fragmentation of cells and positive hematoxylin counterstaining. Normal liver tissue showed no HIF-1 α staining (Figure 5a).

VX2 liver tumors showed areas of HIF-1 α positive staining. A characteristic pattern of HIF-1 α staining was observed in the post- TAE whole tumor specimen slides. HIF-1 α staining was seen to be maximum at the junction of the necrotic and the viable tumor tissue and was observed in all the tumors (Figure 5b, 5c). TAE of liver tumors resulted in a statistically significant increase in the mean percentage of HIF-1 α expression. The mean percentage of HIF-1 α positive stained nuclei increased from 23 % ± 3.5% in pre- TAE biopsy specimens to 41% ± 8.7% ($p< 0.02$) in post- TAE biopsy specimens. The increase was even more significant when mean percentage of HIF-1 α positive stained nuclei from the same pre- TAE biopsy specimens were compared to sections from post- TAE whole tumor specimens [60% ± 8.9% ($p<0.02$)] (Figure 6, 7).

Discussion

In our study, we successfully demonstrated statistically significant increased levels of mean HIF-1 α expression after TAE in same rabbit VX2 liver tumors. The mean percentage of HIF-1 α expression in VX2 tumors increased from 23% before TAE to 41% (sampled tumor) and 60% (whole tumors) after TAE ($p<0.02$). The likely mechanism for the up-regulation of HIF-1 α after embolization is through hypoxia and ischemia of viable tumor tissues.

HIF-1 α is expressed in malignant tumors of the prostate, colon, breast, lung, kidney and liver and has been associated with an increased mortality and treatment failures (11,16–18). Most of these pre-clinical studies have examined the effect of transient disruption of blood supply to targeted tissue. However, the role of HIF-1 α in HCC, especially its behavior after TAE, remains poorly understood.

In a recent publication, Rhee et al (11) demonstrated absence of HIF-1 α expression in normal rabbit liver parenchyma and a significant increase in HIF-1 α expression in targeted VX2 liver tumors that underwent embolization. However the control arm of their study employed VX2 tumors in different rabbits that did not undergo embolization. They also evaluated the HIF-1 α levels 2hrs post- TAE as compared to our study where the post-TAE biopsies were taken at 10 min. In another recent study, Bozova et al (10) showed that in an experimental liver fibrogenesis model in Wistar rats, HIF-1 α expression gradually increased as the severity of cirrhosis increased and correlated strongly with the VEGF expression and angiogenesis. We are unaware of any published studies which have evaluated HIF-1 α expression within the same tumor before and after TAE / TACE. This gap in knowledge motivated us to undertake the current study in which we have shown that TAE increases HIF-1 α expression within the same embolized tumor.

HIF-1 α has been shown to have a half-life of approximately 5 min in normoxic conditions (19,20). As the cells are exposed to hypoxic conditions, HIF-1 α is protected from ubiquitination and is translocated to nucleus. Jewell et al (20), showed that induction of HIF-1 α in response to hypoxia is instantaneous and were able to detect its level in the nucleus of the cells after less than 2 min exposure to hypoxia. This prompted us to select a 10 min time period after TAE to ensure detection of HIF-1 α expression, if any should be present, within the VX2

liver tumors. Had we selected further time points beyond 10 min interval after embolization, we postulate that there might have been an even greater expression of HIF-1 α.

Our study had several important limitations. First, we studied only one end point for all the 7 VX2 liver tumors: complete "stasis" of antegrade blood flow, i.e. SACE level IV. Sub-stasis endpoints, defined as SACE levels I – III (15), might be expected to induce lesser degrees of HIF-1 α expression. Second, we evaluated the post- TAE HIF-1 α expression for all the rabbits at one fixed time point, i.e. 10 min after each embolization. It is possible that varying degrees of expression might occur at different time points. Third, we did not assess alternative techniques that are used to treat HCC, such as chemo- or radio-embolization. The effects of employing alternative "sub-stasis" end points, assessing HIF-1 α levels at serial time points, and performing chemo- or radio-embolizations are a subject of future study. Fourth, the HIF-1 α levels in the center or periphery of the tumor may vary and this may have added a sampling bias when we took the pre- and post- TAE biopsies from the tumors. However, we attempted to reduce these potential errors by taking multiple biopsies from the periphery of all 7 tumors where most of the viable tumor tissue would be expected. To further minimize the sampling bias and to eliminate any possible influence of pre-TAE biopsies on post- TAE biopsy specimens, HIF-1 α levels in the pre-TAE biopsy specimens were compared separately to the post- TAE whole tumors. Finally, due to a limited amount of biopsy material, we restricted analysis of HIF-1 α levels to immunohistochemistry and did not verify results with other quantitative biochemical methods, such as Western blot, RT-PCR or immunoprecipitation.

In conclusion, TAE of VX2 liver tumors up-regulates HIF-1 α, a transcription factor that in turn regulates other pro-angiogenic factors. This expression could be a cause for tumor angiogenesis associated with some treatment failures. Future studies should seek to confirm similar results in clinical patients. The results of these studies might be helpful to target optimal embolization endpoints that maximize necrosis and minimize induction of tumor angiogenic factors. They could also help determine clinical settings where the addition of anti-angiogenic therapy to TAE / TACE might be considered.

Acknowledgements

The authors wish to thank Kathleen R. Harris and Dr. Richard Tang in the Department of Radiology, Northwestern University, for their assistance in all aspects of animal care and management for this study. The authors would also like to thank Robert H. Lurie Comprehensive Cancer Center Pathology Core Facility for their assistance in immunohistochemical HIF-1 α tissue staining. The authors gratefully acknowledge the support of the following grants: American Cancer Society-Illinois Chapter Grant Program, R01CA107467, R01EB002100, and U54CA119341.

RAO was supported in part by the American Cancer Society-Illinois Chapter Grant Program; GW was supported in part by NIH U54 CA119341, P50 CA89018, EB 002100 and CA107467

References

1. Llovet JM. Updated treatment approach to hepatocellular carcinoma. J Gastroenterol 2005;40:225–235. [PubMed: 15830281]
2. Llovet JM, Schwartz M, Mazzaferro V. Resection and liver transplantation for hepatocellular carcinoma. Semin Liver Dis 2005;25:181–200. [PubMed: 15918147]
3. Llovet JM, Bruix J. Systematic review of randomized trials for unresectable hepatocellular carcinoma: Chemoembolization improves survival. Hepatology 2003;37:429–442. [PubMed: 12540794]
4. Liao XF, Yi JL, Li XR, Deng W, Yang ZF, Tian G. Angiogenesis in rabbit hepatic tumor after transcatheter arterial embolization. World J Gastroenterol 2004;10:1885–1889. [PubMed: 15222029]
5. Seki T, Tamai T, Ikeda K, et al. Rapid progression of hepatocellular carcinoma after transcatheter arterial chemoembolization and percutaneous radiofrequency ablation in the primary tumour region. Eur J Gastroenterol Hepatol 2001;13:291–294. [PubMed: 11293452]

6. Kim KR, Moon HE, Kim KW. Hypoxia-induced angiogenesis in human hepatocellular carcinoma. J Mol Med 2002;80:703–714. [PubMed: 12436347]
7. Wu XZ, Xie GR, Chen D. Hypoxia and hepatocellular carcinoma: The therapeutic target for hepatocellular carcinoma. J Gastroenterol Hepatol 2007;22:1178–1182. [PubMed: 17559361]
8. Semenza GL, Wang GL. A nuclear factor induced by hypoxia via de novo protein synthesis binds to the human erythropoietin gene enhancer at a site required for transcriptional activation. Mol Cell Biol 1992;12:5447–5454. [PubMed: 1448077]
9. Sun HC, Tang ZY. Angiogenesis in hepatocellular carcinoma: the retrospectives and perspectives. J Cancer Res Clin Oncol 2004;130:307–319. [PubMed: 15034787]
10. Bozova S, Elpek GO. Hypoxia-inducible factor-1alpha expression in experimental cirrhosis: correlation with vascular endothelial growth factor expression and angiogenesis. Apmis 2007;115:795–801. [PubMed: 17614845]
11. Rhee TK, Young JY, Larson AC, et al. Effect of transcatheter arterial embolization on levels of hypoxia-inducible factor-1alpha in rabbit VX2 liver tumors. J Vasc Interv Radiol 2007;18:639–645. [PubMed: 17494846]
12. Virmani S, Wang D, Harris KR, et al. Comparison of transcatheter intraarterial perfusion MR imaging and fluorescent microsphere perfusion measurements during transcatheter arterial embolization of rabbit liver tumors. J Vasc Interv Radiol 2007;18:1280–1286. [PubMed: 17911519]
13. Virmani S, Harris KR, Szolc-Kowalska B, et al. Comparison of Two Different Methods for Inoculating VX2 Tumors in Rabbit Livers and Hind Limbs. J Vasc Interv Radiol 2008;19:931–936. [PubMed: 18503910]
14. Laurent A, Wassef M, Chapot R, et al. Partition of calibrated tris-acryl gelatin microspheres in the arterial vasculature of embolized nasopharyngeal angiofibromas and paragangliomas. J Vasc Interv Radiol 2005;16:507–513. [PubMed: 15802450]
15. Lewandowski RJ, Wang D, Gehl J, et al. A comparison of chemoembolization endpoints using angiographic versus transcatheter intraarterial perfusion/MR imaging monitoring. J Vasc Interv Radiol 2007;18:1249–1257. [PubMed: 17911515]
16. Huang GW, Yang LY, Lu WQ. Expression of hypoxia-inducible factor 1alpha and vascular endothelial growth factor in hepatocellular carcinoma: Impact on neovascularization and survival. World J Gastroenterol 2005;11:1705–1708. [PubMed: 15786555]
17. Talks KL, Turley H, Gatter KC, et al. The expression and distribution of the hypoxia-inducible factors HIF-1alpha and HIF-2alpha in normal human tissues, cancers, and tumor-associated macrophages. Am J Pathol 2000;157:411–421. [PubMed: 10934146]
18. Zhong H, De Marzo AM, Laughner E, et al. Overexpression of hypoxia-inducible factor 1alpha in common human cancers and their metastases. Cancer Res 1999;59:5830–5835. [PubMed: 10582706]
19. Huang LE, Gu J, Schau M, Bunn HF. Regulation of hypoxia-inducible factor 1alpha is mediated by an O2-dependent degradation domain via the ubiquitin-proteasome pathway. Proc Natl Acad Sci U S A 1998;95:7987–7992. [PubMed: 9653127]
20. Jewell UR, Kvietikova I, Scheid A, Bauer C, Wenger RH, Gassmann M. Induction of HIF-1alpha in response to hypoxia is instantaneous. Faseb J 2001;15:1312–1314. [PubMed: 11344124]

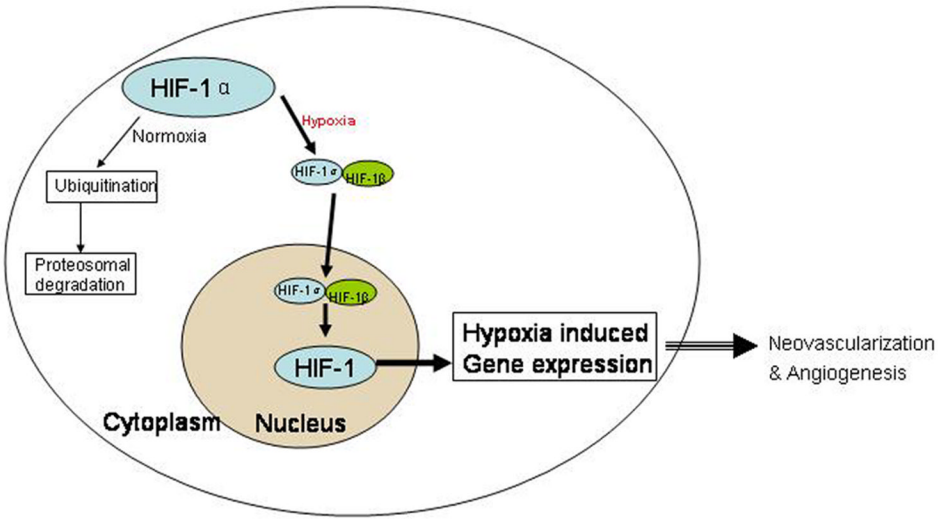

Figure 1.

HIF-1 α activity under normoxic and hypoxic conditions. HIF-1 is a major transcription factor that is composed of two subunits: HIF-1 α and HIF-1 β (beta). Under normoxic conditions, HIF-1 β is constitutively expressed and HIF-1 α is targeted to proteosomal degradation via ubiquitination. On the other hand during hypoxic conditions when oxygen concentration is low, HIF-1 α is stabilized and translocates to nucleus, where it dimerizes with HIF-1 β to form functional HIF-1. This altered redox state occurring in the cells experiencing hypoxia in turn indicates gene transcription of several angiogenic factors.

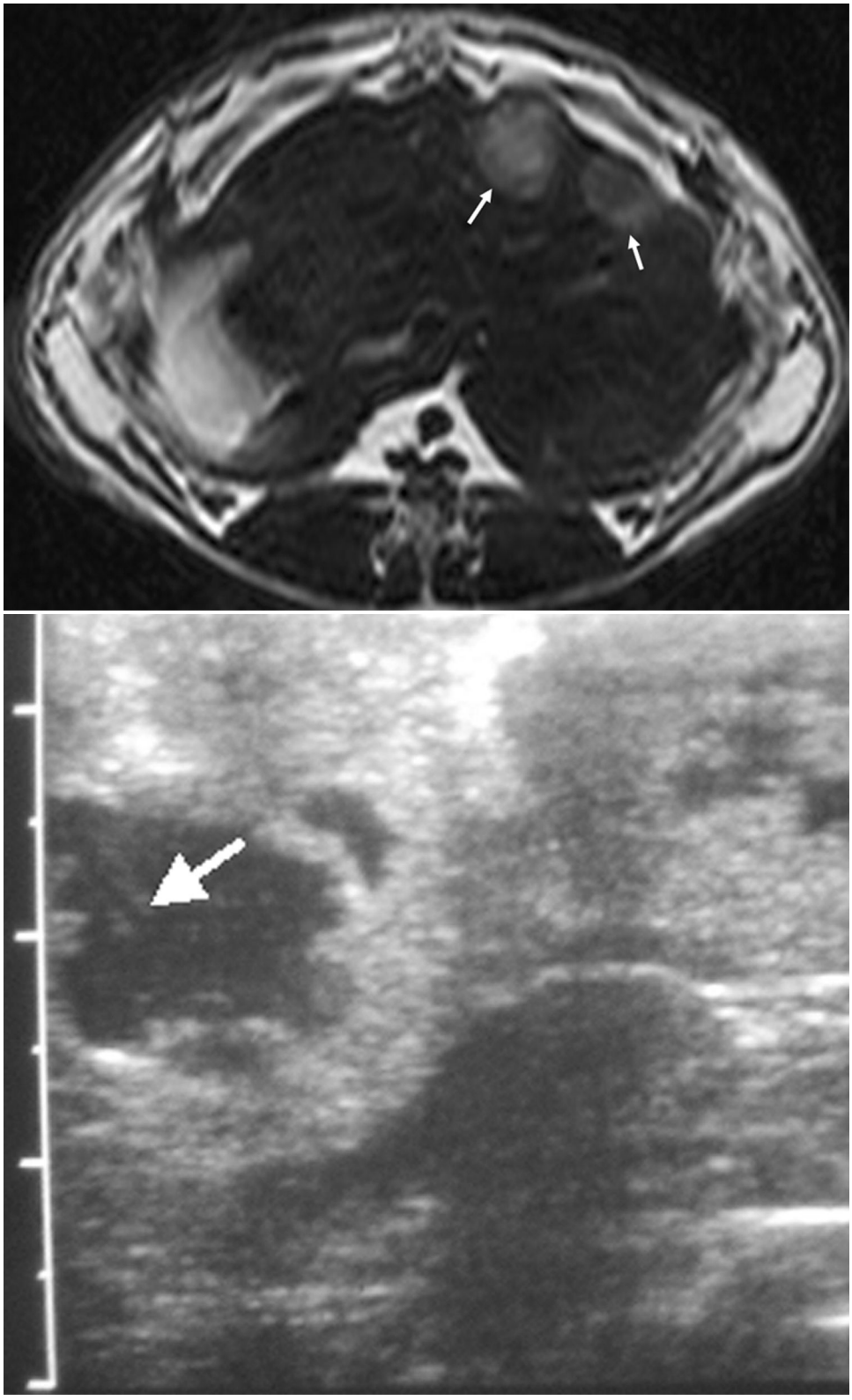

Figure 2.

(a) Axial T2-w MR image showing two VX2 tumor foci in the rabbit's liver. Tumors show increased signal intensity (arrows) relative to remaining liver; **(b)** abdominal ultrasound of the rabbit liver showing a hypo-echoic tumor. Also seen is the biopsy needle (arrow) at the center of the tumor.

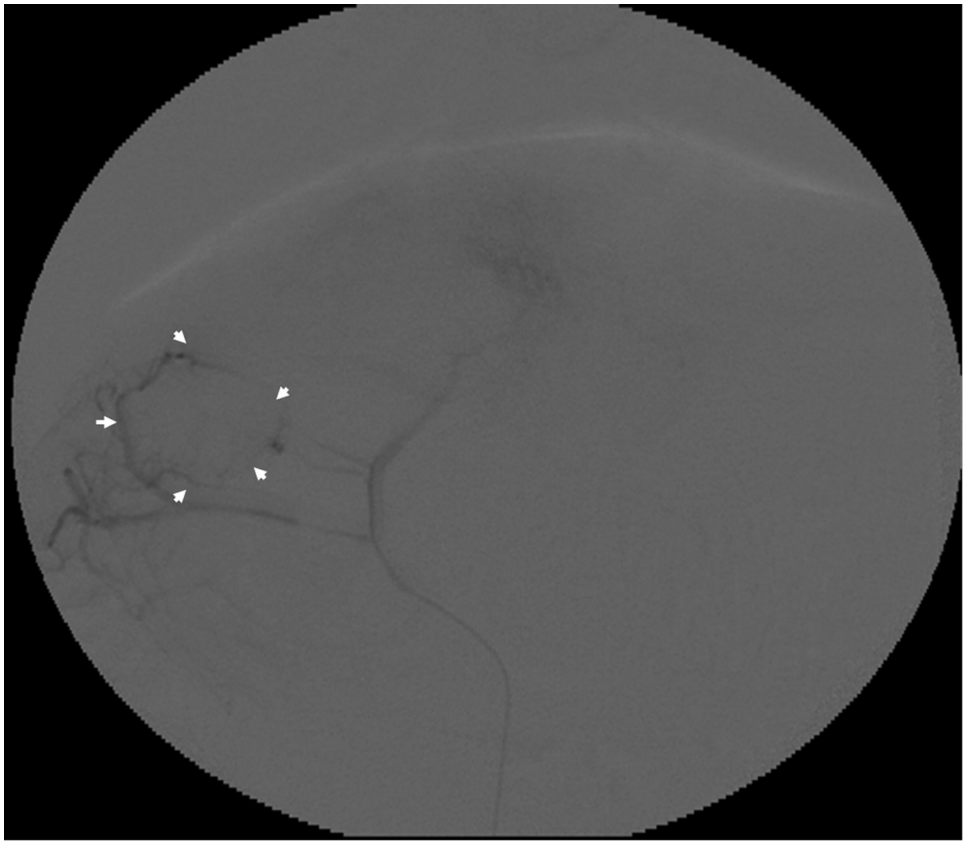

Figure 3.
Representative rabbit hepatic arteriograms before **(a)** and after **(b)** embolization of the left hepatic artery, which supplied the targeted VX2 liver tumor. The peripheral portion of the tumor is hypervascular (white arrows) prior to embolization **(a)**. After embolization **(b)** there is abrupt cut off (black arrow) of the feeding artery without any remaining peripheral hypervascularity.

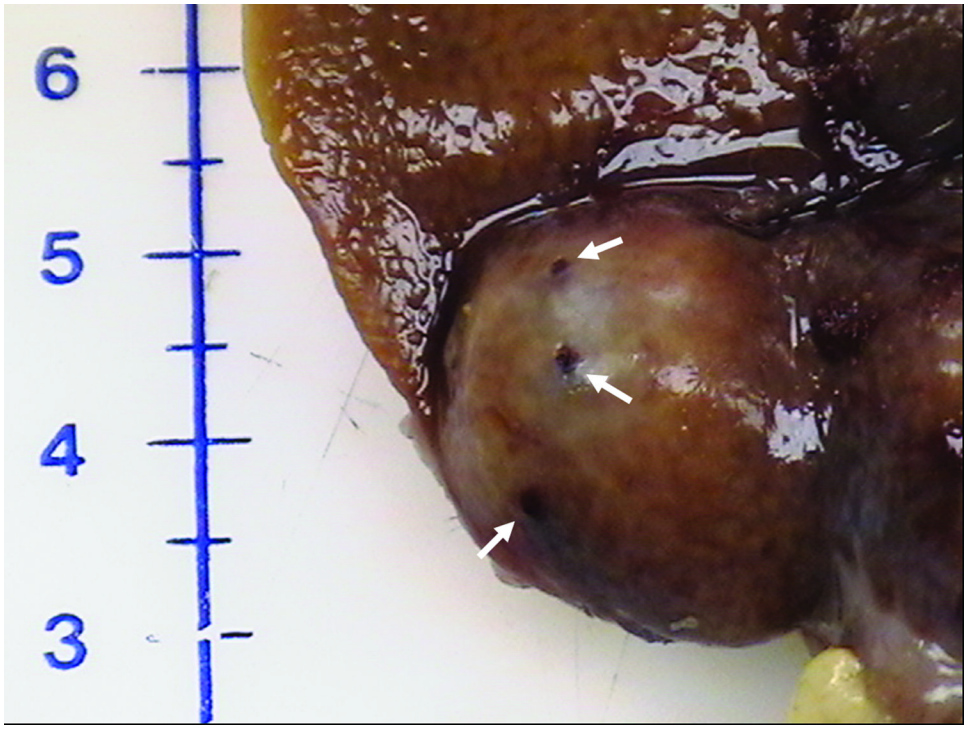

Figure 4.
Harvested rabbit VX2 Liver tumor. Photograph showing multiple biopsy needle puncture sites (arrows) on the tumor surface. No evidence of any significant surrounding hemorrhage can be seen.

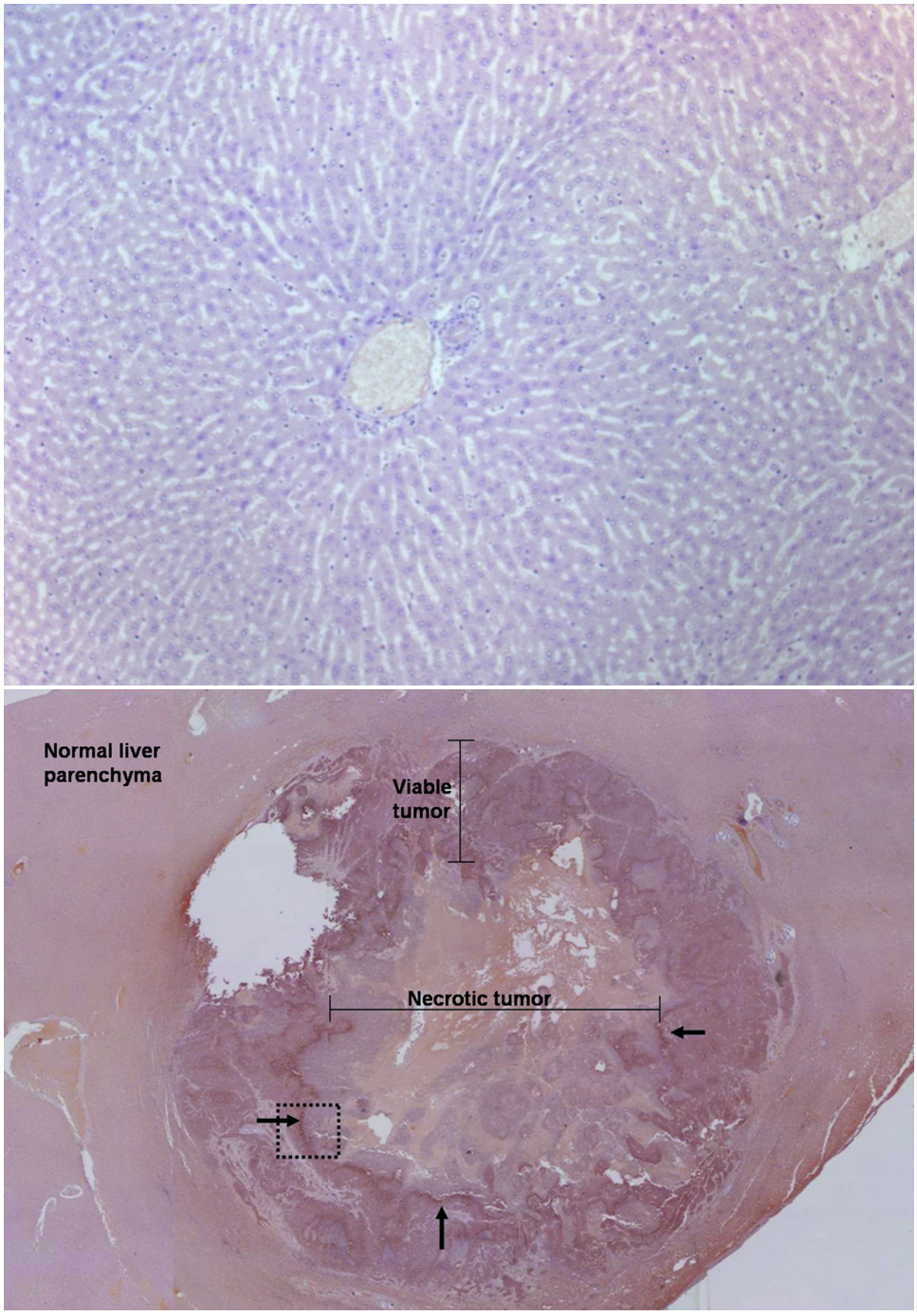

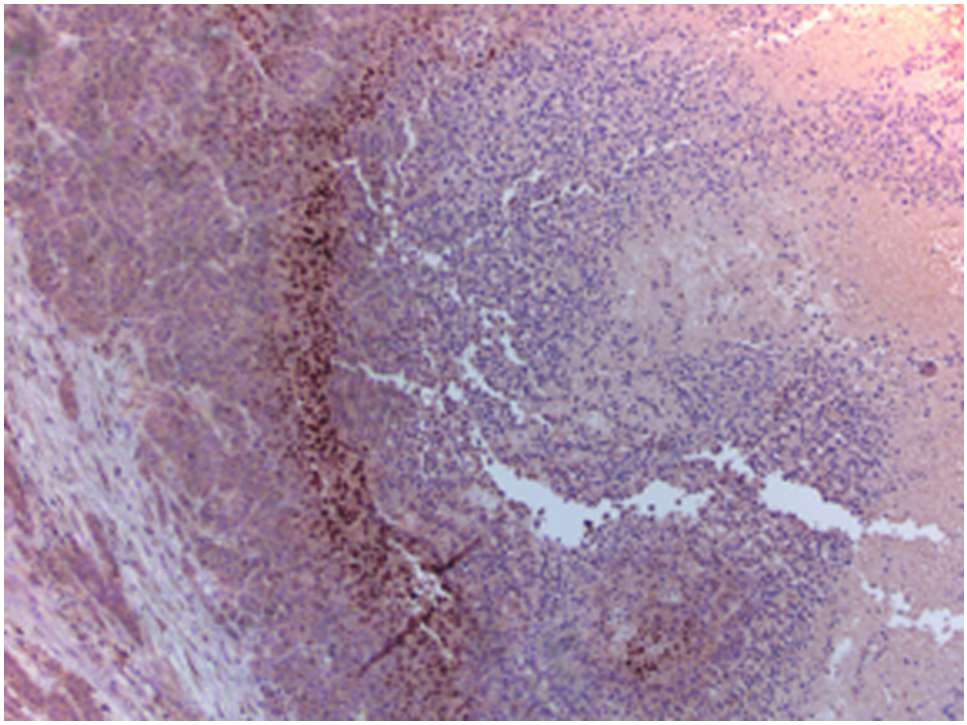

Figure 5.

Immunohistochemical staining: **(a)** High-power photomicrograph (original magnification, X 20) of normal liver parenchyma adjacent to VX2 tumor (post-TAE) showing absence of HIF-1 α staining in these cells. **(b)** High-power photomicrograph (original magnification, X 2.5) of the whole tumor (post- TAE) showing the maximum intensity of HIF-1 α staining at the junction of the necrotic and the viable tumor tissue. Images were stitched together using Canon PhotoStitch 3.1 software. **(c)** High-power photomicrograph (original magnification, X 10) showing the dark brown nuclear staining, positive for the presence of HIF-1 α staining in these cells.

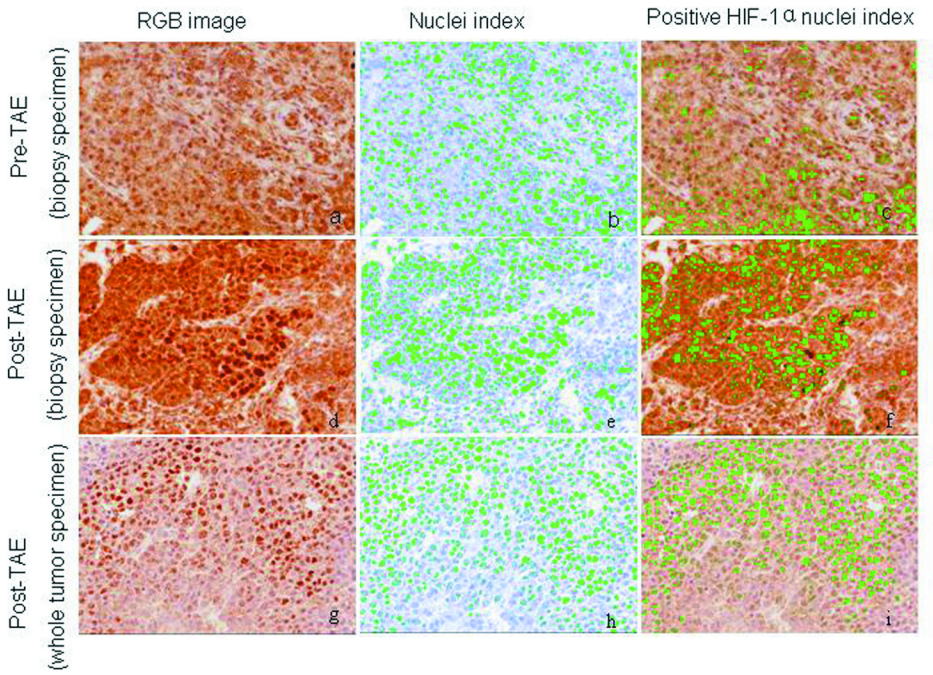

Figure 6.

Immunohistochemical staining for HIF-1α. Pre- TAE (biopsy specimen), post- TAE (biopsy specimen) and post- TAE (whole tumor specimen) were analyzed for percentage of HIF-1 α positive nuclei using the Nuance spectral unmixing system. After obtaining the RGB images (images **a, d** and **g**), nuclei / HPF were counted (images: **b, e** and **h**) using the software (marked green) and then analyzed for nuclei with positive HIF-1α staining (marked green) (images **c, f** and **i**). TAE of liver tumors resulted in a statistically significant increase in the mean percentage of HIF-1 α expression.

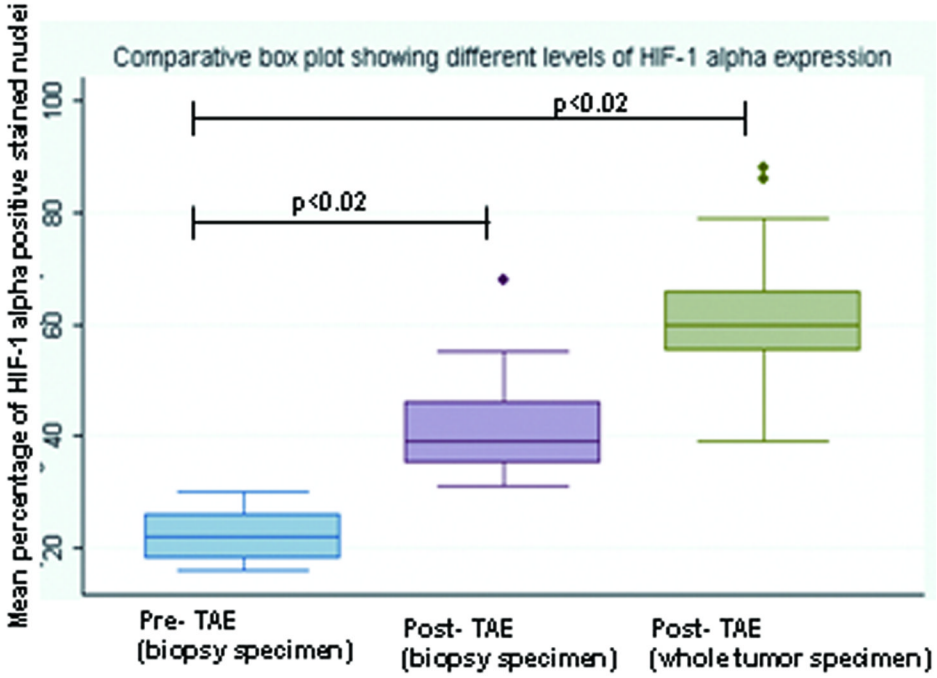

Figure 7.

Box plot showing different levels of HIF-1 α expression in the pre- TAE (biopsy specimen), post- TAE (biopsy specimen) and post- TAE (whole tumor specimen). The boxes represent the inter-quartile range (IQR), the line across the box indicates the median and lines extending from the box represent the 1.5 times the IQR. Values outside the IQR represent the outliers.